ELSEVIER

Surface Science 340 (1995) L960–L964

surface science

Surface Science Letters

Ostwald ripening of vacancy islands at thiol covered Au(111)

Ornella Cavalleri, Andreas Hirstein, Klaus Kern *

Institut de Physique Expérimentale, EPF Lausanne, CH-1015 Lausanne, Switzerland

Received 17 April 1995; accepted for publication 27 June 1995

Abstract

The growth kinetics of vacancy islands at a Au(111) surface covered with self-assembled thiol monolayers has been investigated by in-situ scanning tunneling microscopy. The vacancy islands are found to coarsen by Ostwald ripening. The exponent characterizing the power-law time dependence of the coarsening is found to be $n \approx 1/2$ independent of the thiol chain length ($CH_3(CH_2)_xSH$, $x = 5, 9, 17$). This behavior is consistent with a model in which the mass transport is limited by the adsorption/desorption rate of vacancies at the hole edges.

Keywords: Gold; Growth; Scanning tunneling microscopy; Self-assembly; Surface defects; Surface morphology; Thiols

Because of their interest in both fundamental research and technological applications, self-assembled monolayers are currently object of intense investigations. The most widely studied systems are *n*-alkanethiol monolayers chemisorbed on Au(111). Several characterization techniques like infrared spectroscopy, electron X-ray, thermal helium diffraction and scanning probe microscopy have shown that these molecules self-assemble on Au(111) forming compact monolayers with an average tilt of the molecular axis of $\sim 30°$ with respect to the normal to the surface [1]. On the microscopic scale the thiol monolayers have been found to be ordered in different molecular superstructures with 4 molecules per unit cell [2–5]. Coherent molecular superstructure domains are measured to extend over several hundred Å and the various superstructures are attributed to different molecular conformational orderings.

On the mesoscopic scale, scanning probe microscopy (STM and AFM) has revealed the presence of peculiar defects at the thiol/Au(111) interface. After the thiol chemisorption (self-assembly), the sample surface presents small depressions a few nm in size, 0.2–0.3 nm in depth, which are not observed on bare gold. These pits are vacancy islands in the topmost layer of the gold substrate [6] caused by the dissolution of gold through a gold–thiol complex formation accompanying the self-assembly process. Different observations confirm the substrate origin of these depressions: the molecular superstructure has been observed also inside the holes [7], the pit depth is independent of the thiol chain length [6,7] and amounts of gold have been revealed in the thiol solution after the substrate immersion [8,9].

Notwithstanding the great amount of studies which have been done on these systems, the attention has generally been focused on the molecular structure of the monolayer which, once formed, has been viewed as largely immobile. Only a few investigations have

* Corresponding author. Fax: +41 21 693 3604.

SSDI 0039-6028(95)00790-3

been done to study the stability of the monolayer, e.g. collective properties and mass transport in these systems after chemisorption. In particular, recent STM investigations have shown that heating the thiol monolayer up to 350–370 K causes the vacancy defects to be healed out [6,10] leaving perfectly flat depression-free self-assembled monolayers.

In the present Letter we report on in-situ STM studies of the coarsening kinetics (i.e. the initial stage of the healing process) of the vacancy defects at the alkanethiol/Au(111) interface. We show that, at elevated temperature (320–360 K), the average vacancy island radius grows in size according to the power law scaling $r \propto t^n$, where $n \approx 1/2$ and t is the observation time referred to the time at which the sample reaches the new temperature. The power-law behavior is consistent with a coarsening model due to Ostwald ripening.

Following the classical approach of Lifshitz and Slyozov [11] and Wagner [12] for the growth of three-dimensional clusters in solution, the kinetics of mass flow accompanying the growth of two-dimensional clusters on a surface can be described in a similar way as the result of mainly two processes: the adsorption/desorption of an adatom at the edge of a cluster and the two-dimensional diffusion of the adatoms on the terraces. The same model can also be applied to the mass transport accompanying the growth of two-dimensional vacancy islands on a surface. According to this approach the equilibrium concentration of monovacancies at the edge of a pit depends on the pit radius r according to the Gibbs–Thomson relation $c_{eq} = c_\infty \, e^{\gamma\Omega/rk_bT}$, where c_∞ is the equilibrium concentration of vacancies near a straight step edge, γ is the step edge free energy and Ω is the area of the surface occupied by a vacancy. The Gibbs–Thomson relation implies that the equilibrium concentration is greater at the edge of a small pit than at the edge of a larger one. As a consequence the evaporation rate of vacancies will be faster at the edge of small holes than at the edge of large ones. The second process which contributes to the mass transport is the two-dimensional, concentration gradient driven, diffusion of vacancies away from high curvature pit boundaries towards less curved step egdes. Each of these two processes has its proper activation barrier and for each examined system the resulting kinetic behavior depends on the energetic balance between the two processes at the microscopic level.

Depending on which of the two processes is the rate-limiting step for the mass flow a different power is obtained in the scaling law $r \propto t^n$ [13]. If the evaporation rate of vacancies from the pit edge is faster than the diffusion rate, then diffusion is the limiting step in the mass flow and $n = 1/3$. On the other hand, if the detachment rate of vacancies is the limiting process in the mass transport the exponent is $1/2$.

In the present experiment thiols of different chain length (hexanethiol $CH_3(CH_2)_5SH$, decanethiol $CH_3(CH_2)_9Sh$, octadecanethiol $CH_3(CH_2)_{17}SH$) were deposited on gold films epitaxially grown on mica. The gold substrates were prepared by vacuum deposition of 1000 Å thick gold films onto mica sheets preheated at 550 K. Gold films were flame-annealed in a butane-oxygen flame and quenched in ethanol. STM investigations revealed the presence of large 100–300 nm wide, defect-free terraces separated mostly by monatomic steps. The surfaces were of the (111)-type, as could be inferred from atomic resolution images, and showed the herringbone reconstruction patterns [14]. To prevent any contamination of the samples, the gold substrates were flame-annealed, immediately quenched in ethanol and, while still covered with an ethanol droplet, transferred into a 1mM ethanol solution of thiols. The self-assembled monolayers were prepared by keeping the substrates in the thiol solution for several hours (typically 20 h) at room temperature and final copious rinsing with ethanol. Only highest quality products from Fluka and high purity, low water content ethanol were used. The STM experiments were performed with a home-built "beetle-type" microscope. This stand along STM configuration permits an easy thermal coupling of the sample holder to a Peltier element and because of its inherent thermal self-compensation this microscope is particularly suited for in-situ variable temperature studies [15]. In order to study the thermal behavior of the self-assembled monolayers, we performed isothermic STM measurements at elevated temperatures (320–360 K). These experiments were done under controlled atmosphere by continuous flushing of the microscope compartment with dry nitrogen gas.

The as-prepared thiol–Au(111) interfaces showed

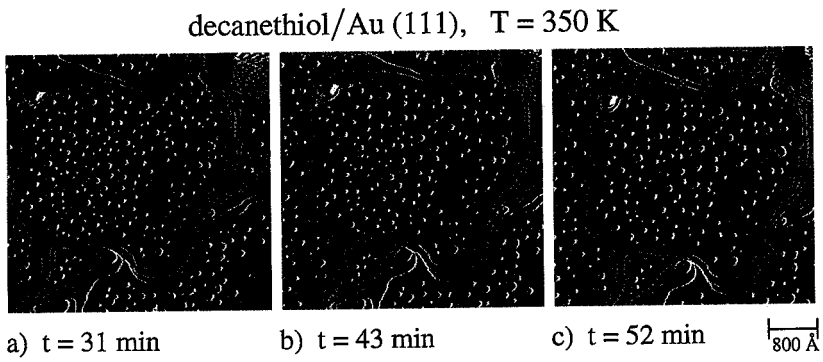

Fig. 1. Temporal development of the morphology of the decanethiol-covered Au(111) surface during annealing at 350 K. All STM images span 4300 Å × 4300 Å.

the well known morphology with the high density of substrate vacancy defects a few nanometer in size and one monolayer in depth [6–10]. These substrates pits are the result of a chemical erosion process accompanying the self-assembly of the organic layer. A large part of the eroded gold atoms dissolves into solution. Gold readsorbing from the solution to the substrate is immediately attached to prexisting substrate steps due to its high lateral mobility at room temperature.

In Fig. 1 we report a time-lapse sequence of STM images characterizing the initial heating of a decanethiol-covered Au(111) surface. The sample was heated in-situ at 345 K and the images were acquired at the same temperature. Figs. 1a–1c show the same area of the surface 31, 43 and 52 min after the temperature raising, respectively. The images were recorded in differential mode, which means that the derivative of the line of constant current is recorded. Typical tunneling parameters were 1 V and 0.5 nA. As can be inferred from the comparison between the three images, the number of vacancy islands decreases with time, while the average hole size increases. In the absence of annihilation at steps the total defect area remains constant as can be shown by an analysis on sufficiently large terraces far away from substrate steps. Similar sequences of images have been obtained on hexanethiol and octadecanethiol monolayers. It must be noted that this mass transport observation is not an artifact caused by tip scanning as can be assured by observing that regions which have not been subject to repeated imaging show the same behavior.

In the following we present the results of a quantitative analysis of the vacancy island growth kinetics for Au(111) surfaces covered with hexane-, decane- and octadecanethiol monolayers. All the data have been taken from surface regions where no annihilation of defects occurred. The graph of Fig. 2a refers to the data obtained on a hexanethiol monolayer and reports, in logarithmic scale, the average vacancy island area, in arbitrary units, versus the observation

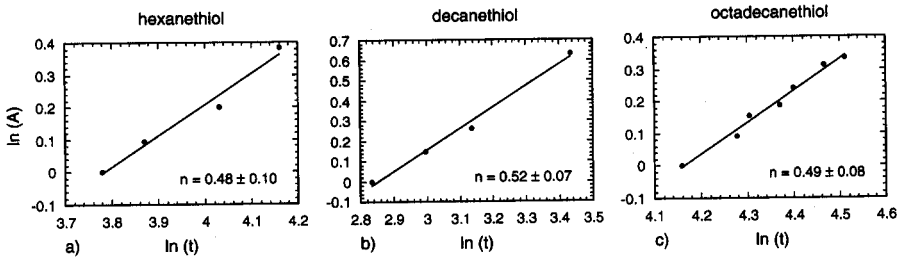

Fig. 2. Temporal variation of the average vacancy island size of thiol-covered Au(111). (a) Hexanethiol, annealing temperature 325 K, (b) decanethiol, annealing temperature 350 K and (c) octadecanethiol, annealing temperature 345 K.

time (in min), the origin of which is choosen in correspondance of the temperature raising. The dependence of $\ln(A)$ on $\ln(t)$ is linear with a unitary angular coefficient. This means that the average pit size scales with time according to the power law $r \propto t^n$, with $n = 0.48 \pm 0.10$. The same analysis performed on different hexanethiol samples gave results comprised in the range 0.4–0.6. Analogous results were obtained on decane- and octadecanethiol monolayers. The graphs in Figs. 2b and 2c refer to two series of images obtained on decane- and octadecanethiol-covered Au(111), determining exponents of $n = 0.52 \pm 0.07$ and 0.49 ± 0.08, respectively.

Since in the early stage of growth described here coalescence does not contribute we can assume that the mass transfer happens either (1) via exclusive intralayer diffusion of monovacancies detaching from smaller holes and readsorbing at larger ones or (2) via the diffusion of Au adatoms at the upper terrace which are emitted through uphill interlayer diffusion at the larger holes and reincorporated (downhill interlayer diffusion) at the edge of smaller ones. At 350 K, however, the latter possibility can be excluded because the emission channel will not be populated due to the high energy barrier for the uphill interlayer diffusion [16]. This leads us to conclude that the hole coarsening process is the result of intralayer diffusion of vacancies.

The observed growth kinetics with exponent $n = 1/2$ is in agreement with this conclusion and suggests that, independently of the chain length, the intralayer mass transport of the vacancy islands at thiol-covered Au(111) surfaces is a process governed by the adsorption/desorption rate of monovacancies at the pit edges. It is interesting to note that an analogous behavior was found for gold adcluster coarsening on impurity-covered Au(111). Peale et al. [17] also found in this system the adsorption/desorption rate of adatoms at the cluster edges to be the rate-determining process.

In the kinetic analysis we have only included data with annealing temperatures $T \leqslant 350$ K and annealing times below about 90 min in order to minimize the influence of coalescence. Deviations are expected from the power law coarsening kinetics when coalescence dominates or contributes substantially to the dynamics of the system. In our experiments we have found coalescence to be negligible in the initial

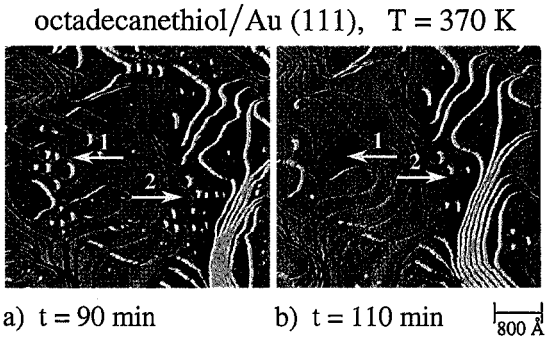

Fig. 3. Edge annihilation and coalescence in the late-stage evolution of vacancy islands at octadecanethiol-covered Au(111). The sample has been annealed 90 min (a) and 110 min (b) at 370 K. All STM images span 4480 Å × 4480 Å.

growth stage. Only in the late-stage growth, coalescence becomes increasingly important. Indeed, it is only the dynamical coalescence and the dynamical annihilation of pits at preexisting steps which render the complete healing of the vacancy defects possible [6]. This is illustrated in Fig. 3 for octadecanethiol-covered Au(111). The two STM images show the late-stage evolution of the film morphology after 90 min and 110 min annealing at 370 K. On the left hand side several vacancy islands on the topmost gold layer (arrow 1) are annihilated at preexisting Au(111) step edges. On the low terrace on the right hand side (arrow 2) we notice the coalescence of neighboring vacancy islands.

Although the kinetic growth law of the vacancy mass flow does not depend on the thiol chain length, the mass flow rate has been found to be chain length dependent. Fig. 4 shows a hexanethiol- (Fig. 4a) and an octadecanethiol- (Fig. 4b) covered Au(111) surface, which have been annealed at the same temperature (345 K) for the same time (60 min). As can be easily inferred from the comparison of the two images, which are equal in size, the healing process has been faster on the hexanethiol- than on the octadecanethiol-covered gold surface. In Fig. 4a the growth of the vacancy islands has already largely developed and the surface presents a low density of large pits, while in Fig. 4b the surface is still characterized by a high density of small pits.

As can be inferred from the comparison with the results of Peale et al., who analyzed the mass transport process on clean and adsorbate-covered gold

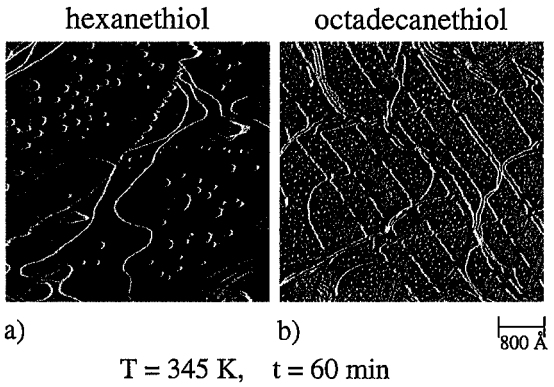

Fig. 4. Morphology of the hexanethiol- (a) and octadecanethiol- (b) covered Au(111) surface after 60 min of annealing at 345 K. The STM image size is 4800 Å×4800 Å.

surfaces, we can conclude that the presence of the monolayer increases the mobility at the gold surface. This increase can be attributed to the lowering of the gold–gold interaction due to the strong gold–sulfur bonding [18]. The explanation of the dependence of the mass flow rate on the chain length, however, requires further studies on the molecular mechanisms involved in the process in order to clarify if the mass transport occurs by a movement of the upper layer gold atoms underneath the thiol monolayer or if a displacement of the molecules is also present. However, even if the molecules would not diffuse, the emission and the diffusion of a monovacancy requires at least local rearrangements of thiol molecules which involve inter-chain bond breaking and making. Thus, a higher inter-chain interaction (i.e. a more stable monolayer) is expected to slow down the transport process.

In conclusion, we have studied in-situ the growth kinetics of vacancy islands created during self-assembly of thiol monolayers on Au(111) surfaces. The observed growth kinetics is consistent with an Ostwald ripening mechanism governed by the adsorption/desorption of monovacancies at the pit edges. While the growth law (i.e. the growth mechanism) has been found to be independent of the thiol chain length, the actual growth rate is found to be chain length dependent. In the latest stage of growth coalescence is found to become increasingly important.

Acknowledgements

This research has been sponsored by the Schweizerischer Nationalfonds. We gratefully acknowledge the support of J.P. Bucher in the initial stage of this work.

References

[1] L.H. Dubois and R.G. Nuzzo, Annu. Rev. Phys. Chem. 43 (1992) 437, and references therein.
[2] N. Camillone, Ch.E.D. Chidsey, G.-Y. Liu and G. Scoles, J. Chem. Phys. 98 (1994) 3503.
[3] J.P. Bucher, L. Santesson and K. Kern, Appl. Phys. A 59 (1994) 135.
[4] D. Anselmetti, A. Baratoff, H.-J. Güntherodt, E. Delamarche, B. Michel, Ch. Gerber, H. Kang, H. Wolf and H. Ringsdorf, Europhys. Lett. 27 (1994) 365.
[5] G. Poirier, M.J. Tarlov and H.E. Rusheimer, Langmuir 10 (1994) 3383.
[6] J.P. Bucher, L. Santesson and K. Kern, Langmuir 10 (1994) 979.
[7] C. Schönenberger, J. Sondag-Huethorst, J. Jorritsma and L.G.K. Fokkink, Langmuir 10 (1994) 611.
[8] K. Edinger, A. Golzhauser, K. Demota, C. Wöll and M. Grunze, Langmuir 9 (1993) 4.
[9] J.A.M. Sondag-Huethorst, C. Schönenberger and L.G.K. Fokkink, J. Phys. Chem. 98 (1994) 6826.
[10] R.L. McCarley, R.J. Dunaway and R.J. Willicut, Langmuir 9 (1993) 2775.
[11] I.M. Lifshitz and V.V. Slyozov, J. Phys. Chem. Solids 19 (1961) 35.
[12] C. Wagner, Z. Elektrochem. 65 (1961) 581.
[13] M. Zinke-Allmang, L.C. Feldman and M.H. Grabow, Surf. Sci. Rep. 16 (1992) 377.
[14] J.V. Barth, H. Brune, G. Ertl and R.J. Behm, Phys. Rev. B 42 (1990) 9307.
[15] J.P. Bucher, H. Röder and K. Kern, Surf. Sci. 289 (1993) 370.
[16] G.L. Kellogg, Surf. Sci. Rep. 21 (1994) 1.
[17] D.R. Peale and B.H. Cooper, J. Vac. Sci. Technol. A 10 (1992) 2210.
[18] D.J. Trevor, Ch.E.D. Chidsey and D.N. Loiacono, Phys. Rev. Lett. 62 (1989) 929.